# Gas lines in outbursting young stars as signatures of episodic accretion

Marc Audard[1], A. Postel, E. Vorobyov, O. Dionatos, C. Rab, M. Güdel

1 – University of Geneva, Switzerland

The formation of young stars undergoes episodic, albeit quite common, accretion events in the early life of a young star. The separation of the classical types of outbursting sources, FU Orionis objects and EXor-type objects, has now become blurred thanks to new outbursting sources discovered in the recent past. The physical mechanism (if a common one exists) at the origin of the outbursts still remains unclear. Massive mass transfer through the disk occurs due to episodic accretion, with consequences for planet formation; in addition the strong increase in luminosity can evaporate ices present in the disk. We present our analysis of 12 erupting young stars observed with Herschel and Spitzer (Postel et al. 2019, A&A, 631, A30). The Herschel spectra show many rotational lines of CO, ranging from J=38-37 to J=4-3. Rotational diagrams indicate several excitation temperatures in the low temperature regime (<100K), mid-temperature regime (400-500K) and evidence for a higher temperature component in some cases. Additional lines are detected such as atomic lines (O I, C I, CII, N II), and possibly faint OH and $H_2O$ lines. Spitzer data further reveal several ices in the embedded objects (such as $CO_2$, $CH_3OH$, $NH_4^+$) with silicate in absorption, while at least one target shows silicate in emission, similar to the prototype FU Ori. We present the data in the context of episodic accretion and its signature in emission gas lines, and an analysis of the FUor Re 50 N IRS 1 with the thermochemical code ProDiMo (Postel et al. 2021, submitted).

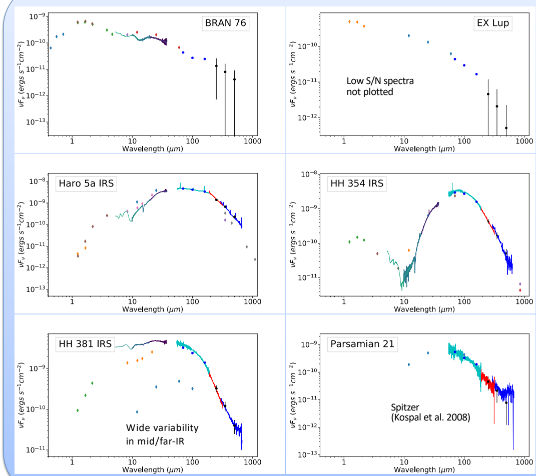


Fig. 1a: The SEDs of the objects BRAN 76 (top left), EX Lupi (top right), Haro 5a IRS (middle left), HH 354 IRS (middle right), HH 381 IRS (bottom left) and Parsamian 21 (bottom right) including PACS spectra and photometry data (turquoise line + blue dots at 70, 100 and 160 μm), SPIRE high resolution spectra (dark blue and red lines) and SPIRE photometry (black dots at 250, 350 and 500 μm) combined with spectra from Spitzer (lines in other colors below 50 μm) and photometry (diamonds; color-grouped by literature) from other sources.

From Postel et al. (2019)

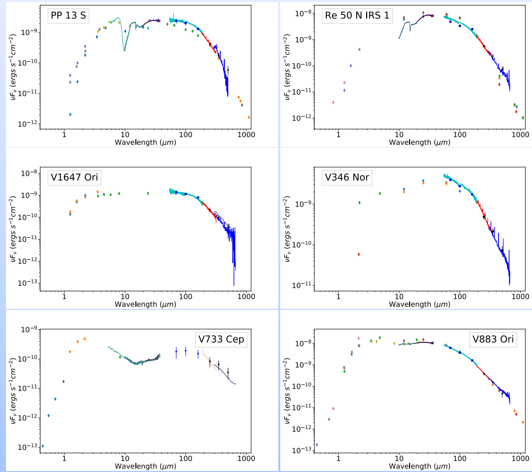


Fig. 1b: The SEDs of the objects PP 13 S (top left), Re 50 N IRS 1 (also known as HBC 494) (top right), V1647 Ori (middle left), V346 Nor (middle right), V733 Cep (bottom left) and V883 Ori (bottom right). Data similar as in Figure 1a. The SED of faint objects (here V1647 Ori and V733 Cep) is complemented with low resolution spectra from SPIRE (thick, orange and purple lines at the same wavelength window as the high-resolution spectra).

From Postel et al. (2019)

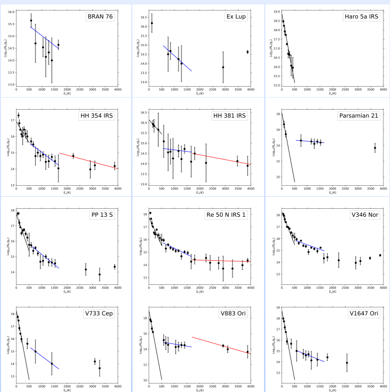


Fig. 2: Left: CO $J$=4-3 to $J$=38-37 rotational diagrams of all objects. We plot the decadic logarithm of the column densities $N_u$ divided by the statistical weight $g_u$, as function of the upper level energy of the transition $E_u$ in Kelvin. SPIRE data are fitted with black, PACS data are fitted with blue and red. As the plots contain a logarithmic scale, the errors are actually not symmetric, but we use it here as an approximation.

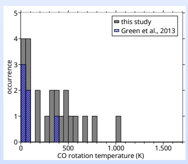


Occurrence of the CO rotation temperatures found in our tar- gets and for V1057 Cyg, V1331 Cyg and V1515 Cyg from Green et al. (2013). Temperatures above 1700 K are not shown here, because of the high uncertainty of the measurements. LTE temperatures of 0-100 K, 400-500 K, and in some cases 1000-2000 K. We confirm the warm component detected in FUors by Green et al. (2013).

From Postel et al. (2019)

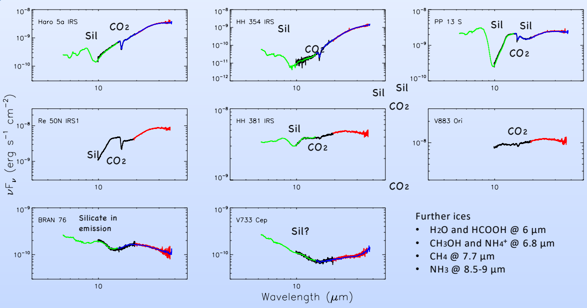


Silicate feature correlates with [O I] luminosity (see also Green et al. 2013)

Fig. 3: Spitzer IRS spectra (5-40μm) showing the high-resolution module SH (black) and LH (red) data and the low-resolution module SL (green) and LL (blue) data. Most FUors in our sample show deep absorption features from silicates (near 10μm and 18μm) and from ices (mainly $CO_2$, $H_2O$, $CH_3OH$). Some gas emission lines (mainly [Fe II] at 17.9, 24.5, 26.0, 35.3 μm) are also detected. Note the deep $H_2O$ absorption in Haro 5a IRS, HH 354 IRS, on top of the silicate feature. In contrast $H_2O$ ices are weaker in PP 13 S, Re 50N IRS1, HH 381 IRS, and V883 Ori. Silicate absorption is also weak in HH 381 IRS and V883 Ori. BRAN 76 shows silicate in emission, while V733 Cep shows no evidence of features in absorption or emission. Quanz et al. (2006) also showed this dichotomy of FUors with deep absorption features and strongly increasing SED and other FUors with emission features and flatter infrared slope. From Postel et al. (2019).

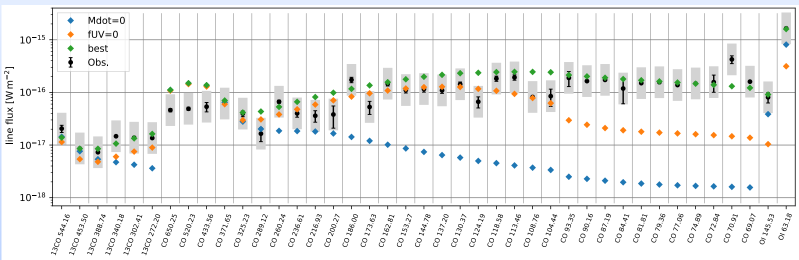


Fig 4: Line fluxes of the best ProDiMo model (green diamonds) compared to a model with disabled disk accretion ($M$ = 4.2 × $10^{-4}$ M⊙ yr−1, $f_{UV}$ = 0, orange diamonds). The best model uses both, disk accretion ($M$ = 6 × $10^{-4}$ M⊙ $yr^{-1}$ and the UV field ($f_{UV}$ = 3%) in combination. The thermo-chemical model ProDiMo was adapted by Rab et al. (2017) to account for the envelope structure in erupting young stars.

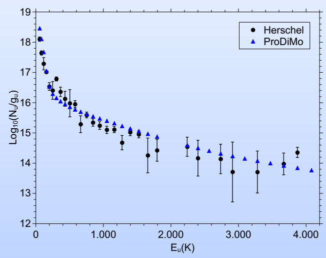


CO rotational diagram for the best model compared to the observational data obtained with Herschel. The gap around 2000 K is caused by a non-detection of the lines in the Herschel data.

From Postel et al. (2021)

•Rab, C., et al. 2017, A&A, 604, 15
•Postel, A., et al. 2019, A&A, 631, A30
•Postel, A., et al. 2021, submitted